Design of Layered Crystalline Materials Using Coordination Chemistry and Hydrogen Bonds

John C. MacDonald,*,† Pieter C. Dorrestein,† Malissa M. Pilley,† Mary M. Foote,† Jaina L. Lundburg,† Robert W. Henning,‡ Arthur J. Schultz,‡ and Jamie L. Manson§

Contribution from the Department of Chemistry, Northern Arizona University, Flagstaff, Arizona 86011-5698, Intense Pulsed Neutron Source and Chemistry and Materials Science Divisions, Argonne National Laboratory, Argonne, Illinois 60439

Received June 12, 2000

Abstract: The supramolecular chemistry and crystal structures of five bis(imidazolium 2,6-pyridinedicarboxylate)M(II) trihydrate complexes, where M = Mn^{2+}, Co^{2+}, Ni^{2+}, Cu^{2+}, or Zn^{2+} (**1**−**5**, respectively), are reported. These complexes serve as supramolecular building blocks that self-assemble when crystallized to generate a single, well-defined, predictable structure in the solid state. 2,6-Pyridinedicarboxylate anions and imidazolium cations form strong ionic hydrogen bonds that dominate crystal packing in compounds **1**−**5** by forming two-dimensional networks, or layers of molecules. This layer motif serves as a platform with which to control and predict molecular packing by design for engineering the structures of crystals. Moreover, compounds **1**−**5** create a robust organic host lattice that accommodates five different transition metals without significantly altering molecular packing. Growth of crystals from solutions that contain two or more different metal complexes produces mixed crystals in which mixtures of the different metal complexes are incorporated in the same relative molar ratio present in solution. Epitaxial growth of crystals from one metal complex on the surface of a seed crystal that contains a second metal complex generates composite crystals in which the different metal complexes are segregated into different regions of the crystals. Compounds **1**−**5** form crystalline solids that represent a new class of modular materials in which the organic ligands serve as a structural component that defines a single packing arrangement that persists over a range of structures, and in which the metal serves as an interchangeable component with which to vary the physical properties of the material.

Introduction

We are exploring a strategy to control structure in the solid state that combines elements of design from two complementary approaches toward crystal engineering. Our goal is to generate supramolecular motifs, or scaffolds, with structures that can be controlled predictably and altered systematically by design. Ultimately, we want to use these scaffolds to produce new materials that are microporous or that exhibit useful optical behavior. The design of crystalline materials, or crystal engineering, is an important and rapidly growing area of research.[1] Recent progress in this area has produced a variety of materials that exhibit a range of physical properties and functionally useful behaviors.[2,3] Currently, the most prevalent strategy for engineering the structures of crystals takes advantage of directional intermolecular interactions between molecules as the principle means of controlling molecular assembly during crystallization.[4,5] For example, the literature is replete with examples of organic crystals in which hydrogen bonds are used to generate supramolecular assemblies of organic molecules with structures that can be controlled selectively in one, two, and three dimensions.[6−8] Crystalline materials composed of organic compounds are attractive from the standpoint of crystal engineering because organic molecules exhibit a wide range of physical properties that are modified easily through synthesis. Although many interesting structures have been discovered, the goal of achieving functional materials from organic crystals has not yet been realized, especially when compared to materials based on organic polymers and inorganic compounds. One potential drawback of purely organic crystals is their relatively low thermal and mechanical stability, which can render them ineffective as materials for devices. Another problem is the tendency of organic compounds with several different functional groups to form more than one pattern of hydrogen bonds, which can promote the formation of polymorphs that have different physical properties.[8−12]

* To whom correspondence should be addressed.
† Northern Arizona University.
‡ Intense Pulsed Neutron Source, Argonne National Laboratory.
§ Chemistry and Materials Science Divisions, Argonne National Laboratory.

(1) Desiraju, G. R. *Crystal Engineering*: *The Design of Organic Solids*; Elsevier: New York, 1989; Vol. 54.
(2) Palmore, G. T. R.; MacDonald, J. C. In *The Amide Linkage*: *Structural Significance in Chemistry, Biochemistry and Materials Science*; Greenberg, A., Breneman, C. M., Liebman, J. F., Eds.; John Wiley and Sons: New York, 2000; pp 291−336.
(3) Vögtle, F. *Supramolecular Chemistry*: *An Introduction*; John Wiley and Sons: New York, 1991.
(4) Aakeröy, C. B.; Seddon, K. R. *Chem. Soc. Rev.* **1993**, 397−407.
(5) Anthony, A.; Desiraju, G. R.; Jetti, R. K. R.; Kuduva, S. S.; Madhavi, N. N. L.; Nangia, A.; Thaimattam, R.; Thalladi, V. R. *Cryst. Eng.* **1998**, *1*, 1−18.
(6) Chin, D. N.; Zerkowski, J. A.; MacDonald, J. C.; Whitesides, G. M. In *Organised Molecular Assemblies in the Solid State*; Whitesell, J. K., Ed.; John Wiley and Sons: New York, 1999; pp 185−253.
(7) Etter, M. C. *J. Phys. Chem.* **1991**, *95*, 4601−4610.
(8) MacDonald, J. C.; Whitesides, G. M. *Chem. Rev.* **1994**, *94*, 2383−2420.
(9) Bernstein, J.; Etter, M. C.; MacDonald, J. C. *J. Chem. Soc., Perkin Trans. 2* **1990**, 695−698.
(10) Bernstein, J. *J. Phys. D*: *Appl. Phys.* **1993**, *26*, B66−B76.
(11) Zerkowski, J. A.; MacDonald, J. C.; Whitesides, G. M. *Chem. Mater.* **1997**, *9*, 1933−1941.

10.1021/ja002102v CCC: $19.00 © 2000 American Chemical Society
Published on Web 11/10/2000

An alternative approach to crystal engineering uses metal−ligand bonds between transition metals and organic ligands to create coordination polymers that have extended structures.[13−23] Coordination compounds have advantages over organic compounds as molecular building blocks because metals exhibit a variety of coordination geometries and a broad range of physical properties that are understood. A potential disadvantage of coordination polymers is that the strength of metal−ligand bonds is typically at least an order of magnitude greater than that of hydrogen bonds. Consequently, the supramolecular structures of some coordination polymers can be very rigid, form irreversibly, and exhibit such fast kinetics for nucleation and growth of crystals that the products form insoluble microcrystalline powders.

Our strategy to control molecular packing in crystalline materials uses strong ionic hydrogen bonds in combination with metal−ligand bonds. This approach provides a means to control the rigidity of a supramolecular framework of molecules joined by metal−ligand interactions by selectively incorporating more flexible hydrogen bonds between molecules. This method should produce large single crystals since hydrogen-bonded structures form reversibly and exhibit slower kinetics for nucleation and growth of crystals than coordination polymers. Moreover, this strategy combines the rich structural and physical chemistry of transition metals with organic compounds to create crystalline materials with potential for optical and microporous applications.[24−29] We have chosen deliberately to work with materials that contain both organic molecules and transition metals not only to control structure, but also to generate materials in which we can induce and manipulate these properties specifically.

This paper describes our efforts to design coordination complexes that self-assemble into two-dimensional supramolecular networks, or layers. We and others have used hydrogen bonds successfully in purely organic crystals to restrict molecular packing to specific one-dimensional motifs (e.g., chains or tapes)[30−40] and two-dimensional motifs (e.g., sheets or layers),[41−50] as shown schematically in Figure 1. Constraining molecules to assemble into layers has several advantages from the standpoint of design and control over bulk crystalline structure: it significantly reduces the degrees of translational freedom available to individual molecules while packing; it limits molecular packing to just a few possible packing arrangements by defining the relative position and orientation of molecules within layers; and it reduces the problem of predicting crystal packing in three dimensions from that of individual molecules to that of well-ordered layers of molecules. To illustrate these advantages, we have shown that hydrogen bonding between imidazolium cations and anions of dicarboxylic acids effectively locks the ions into layers.[51] The anions of

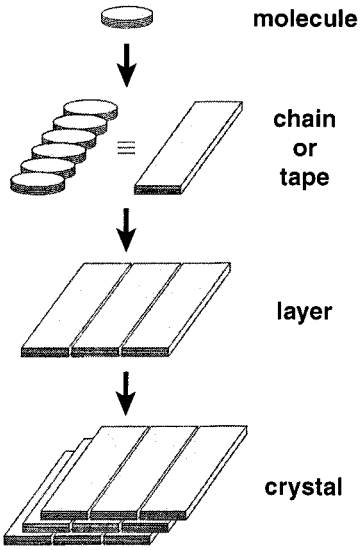

Figure 1. Schematic representation that illustrates how the translational freedom of individual molecules, and thus their packing, can be constrained in one or two dimensions by linking molecules via intermolecular interactions into chains or layers, respectively.

(12) Chin, D. N.; Palmore, G. T. R.; Whitesides, G. M. *J. Am. Chem. Soc.* **1999**, *121*, 2115−2122.
(13) Yaghi, O. M.; Li, G.; Li, H. *Nature* **1995**, *378*, 6558.
(14) Atencio, R.; Biradha, K.; Zaworotko, M. J. *Cryst. Eng.* **1998**, *1*, 203.
(15) Christie, S. D.; Subramanian, S.; Zaworotko, M. J. *J. Chem. Soc., Chem. Commun.* **1994**, 2563.
(16) Li, H.; Davis, C. E.; Yaghi, O. M. *J. Am. Chem. Soc.* **1998**, *120*, 2186.
(17) Munakata, M.; Wu, L. P.; Kuroda-Sowa, T. *Bull. Chem. Soc. Jpn.* **1997**, *70*, 1727−1743.
(18) Sharma, C. V. K.; Rogers, R. D. *Cryst. Eng.* **1998**, *1*, 19−38.
(19) Yaghi, O. M.; Li, H.; Groy, T. L. *J. Am. Chem. Soc.* **1996**, *118*, 9096.
(20) Yaghi, O. M.; Davis, C. E.; Li, H. *J. Am. Chem. Soc.* **1997**, *119*, 2861.
(21) Yaghi, O. M.; Li, H.; Groy, T. L. *Inorg. Chem.* **1997**, *36*, 6.
(22) Yaghi, O. M.; Reinke, T. M.; Eddaoudi, M. *J. Am. Chem. Soc.* **1999**, *121*, 1651.
(23) Zaworotko, M. J. *Chem. Soc. Rev.* **1994**, 283−288.
(24) Aakeröy, C. B.; Beatty, A. M. *Cryst. Eng.* **1998**, *1*, 39−49.
(25) Bailey, R. D.; Hook, L. L.; Powers, A. K.; Hanks, T. W.; Pennington, W. T. *Cryst. Eng.* **1998**, *1*, 51−66.
(26) Bhyrappa, P.; Wilson, S. R.; Suslick, K. S. *J. Am. Chem. Soc.* **1997**, *119*, 8492−8502.
(27) Falvello, L. R.; Pascual, I.; Tomas, M. *Inorg. Chem. Acta* **1995**, *229*, 135−142.
(28) Falvello, L. R.; Pascual, I.; Tomas, M.; Urriolabeitia, E. P. *J. Am. Chem. Soc.* **1997**, *119*, 11894−11902.
(29) Schauer, C. L.; Matwey, E.; Fowler, F. W.; Lauher, J. W. *J. Am. Chem. Soc.* **1997**, *119*, 10245−10246.
(30) Ducharme, Y.; Wuest, J. D. *J. Org. Chem.* **1988**, *53*, 5787−5789.
(31) Foxman, B. M.; Guarrera, D. J.; Taylor, L. D.; VanEngen, D.; Warner, J. C. *Cryst. Eng.* **1998**, *1*, 109−118.
(32) Geib, S. J.; Vicent, C.; Fan, E.; Hamilton, A. D. *Angew. Chem., Int. Ed. Engl.* **1993**, *32*, 119−121.
(33) Karle, I. L.; Rangathanan, D.; Haridas, V. *J. Am. Chem. Soc.* **1997**, *119*, 2777−2783.
(34) Mascal, M.; Fallon, P. S.; Batsanov, A. S.; Heywood, B. R.; Champ, S.; Colclough, M. *J. Chem. Soc., Chem. Commun.* **1995**, 805−806.
(35) Palacin, S.; Chin, D. N.; Simanek, E. E.; MacDonald, J. C.; Whitesides, G. M.; McBride, M. T.; Palmore, G. T. R. *J. Am. Chem. Soc.* **1997**, *119*, 11807−11816.
(36) Schwiebert, K. E.; Chin, D. N.; MacDonald, J. C.; Whitesides, G. M. *J. Am. Chem. Soc.* **1996**, *118*, 4018−4029.
(37) Simanek, E. E.; Tsoi, A.; Wang, C. C. C.; Whitesides, G. M.; McBride, M. T.; Palmore, G. T. R. *Chem. Mater.* **1997**, *9*, 1954−1961.
(38) Toledo, L. M.; Lauher, J. W.; Fowler, F. W. *Chem. Mater.* **1994**, *6*, 1222−1226.
(39) Zerkowski, J. A.; MacDonald, J. C.; Seto, C. T.; Wierda, D. A.; Whitesides, G. M. *J. Am. Chem. Soc.* **1994**, *116*, 2382−2391.
(40) Zerkowski, J. A.; MacDonald, J. C.; Whitesides, G. M. *Chem. Mater.* **1994**, *6*, 1250−1257.
(41) Aakeröy, C. B.; Hughes, D. P.; Nieuwenhuyzen, M. *J. Am. Chem. Soc.* **1996**, *118*, 10134−10140.
(42) Birhadha, K.; Zaworotko, M. J. *Cryst. Eng.* **1998**, *1*, 67−78.
(43) Chang, Y.-L.; West, M.-A.; Fowler, F. W.; Lauher, J. W. *J. Am. Chem. Soc.* **1993**, *115*, 5991−6000.
(44) Coe, S.; Kane, J. J.; Nguyen, T. L.; Toledo, L. M.; Wininger, E.; Fowler, F. W.; Lauher, J. W. *J. Am. Chem. Soc.* **1997**, *119*, 86−93.
(45) Hollingsworth, M. D.; Santarsiero, B. D.; Oumar-Mahamat, H.; Nichols, C. J. *Chem. Mater.* **1991**, *3*, 23−25.
(46) Kane, J. J.; Liao, R.-F.; Lauher, J. W.; Fowler, F. W. *J. Am. Chem. Soc.* **1995**, *117*, 12003−12004.
(47) Karle, I. L.; Ranganathan, D.; Haridas, V. *J. Am. Chem. Soc.* **1996**, *118*, 7128−7133.
(48) Palmore, G. T. R.; McBride, M. T. *Chem. Commun.* **1998**, 145−146.
(49) Pedireddi, V. R.; Chatterjee, S.; Ranganathan, A.; Rao, C. N. R. *J. Am. Chem. Soc.* **1997**, *119*, 10867−10868.
(50) Zhao, X.; Chang, Y.-L.; Fowler, F. W.; Laugher, J. W. *J. Am. Chem. Soc.* **1990**, *112*, 6627−6634.

dicarboxylic acids form hydrogen-bonded chains (O−H···O$^-$) of anions that align in parallel rows. This pattern is prevalent in salts of tartaric and malic acids as well.[52−54] These chains are cross-linked into layers by imidazolium cations that form a second set of hydrogen-bonded chains ($^+$N−H···O$^-$). Layers of this type are ubiquitous in imidazolium carboxylate salts. Moreover, they contain ionic hydrogen bonds that are strong, yet flexible enough to accommodate a range of substituents without disrupting the layer motif. We have used hydrogen bonding between imidazolium cations and carboxylate anions as an element for design in the work described here.

We also describe two novel classes of crystalline materials based on these layered structures. The first class of materials is single crystals that contain two or more different metal complexes that form solid solutions, or mixtures. We refer to these materials as mixed crystals. The second class of materials is single crystals composed of two different regions that contain different metal complexes. We refer to these materials as composite crystals. In the work reported here, emphasis is placed specifically on crystalline structure and molecular packing, the role of coordination chemistry in defining molecular structure, and the role of ionic hydrogen-bonding interactions in defining supramolecular structure. The optical properties of these materials currently are being characterized; their application toward the design of materials that exhibit these properties will be described elsewhere.

Results and Discussion

Layers from Complexes between 2,6-Pyridinedicarboxylic Acid, Imidazole, and First-Row Transition Metals. We have extended the concept of using ionic hydrogen bonds to create layers of molecules from purely organic compounds to complexes that contain both organic molecules and transition metals. Specifically, we have used transition metals in the 2+ oxidation state (e.g. Cu^{2+}) to create coordination compounds that contain two molecules of 2,6-pyridinedicarboxylic acid—a compound that behaves as a tridentate ligand by binding metals at the pyridyl nitrogen and at the two carboxylate groups—and two molecules of imidazole (Figure 2a).[55] These experiments tested the hypothesis that imidazole would form salts with these coordination compounds, and that these salts would assemble into layers. On the basis of our previous work with imidazolium carboxylate salts, we anticipated that the anions would form two sets of hydrogen-bonded chains with imidazolium cations, and that these chains would intersect at the anions, as shown schematically in Figure 2b, to form layers. We also wanted to establish that the organic ligands would dominate the crystal packing and create a host lattice that accommodates different transition metals without significantly altering crystal packing. Crystals that exhibit this characteristic represent a new class of materials in which the organic ligands serve as a structural component that defines a single packing arrangement that persists over a range of structures, and in which the metal serves as an interchangeable component with which to vary the physical properties of the material.

Toward this end we have prepared complexes with several first-row transition metals. Reaction of 2,6-pyridinedicarboxylic acid and imidazole with Mn^{2+}, Co^{2+}, Ni^{2+}, Cu^{2+}, or Zn^{2+} gives the corresponding imidazolium carboxylate metal complexes, **1**−**5**. These complexes form crystals in which the metal atoms are coordinated octahedrally by two ligands of 2,6-pyridinedicarboxylic acid. The resulting salts all contain two imidazolium cations hydrogen bonded to the dianionic metal complex and two molecules of water. These complexes readily form large crystals with well-developed faces and edges. We routinely harvest crystals from solution with dimensions of $5 \times 5 \times 1$ mm^3, although we have grown single crystals as large as $20 \times 20 \times 4$ mm^3. The structures of all the complexes are very similar. Comparison of the molecular structures of the dianions shows that the geometry of the ligands on the metal varies slightly, as shown in Figure 3. Most notably, the N−M−N angle (M = Mn^{2+}, Co^{2+}, Ni^{2+}, Cu^{2+}, or Zn^{2+}) involving the nitrogen atoms on the two pyridyl ligands and the central metal atom varies from bent in the Zn complex [N−Zn−N = 166.2(2)°] to nearly linear in the Cu complex [N−Cu−N = 178.5(7)°]. The N−M−N angles in the remaining metal complexes fall between these values.

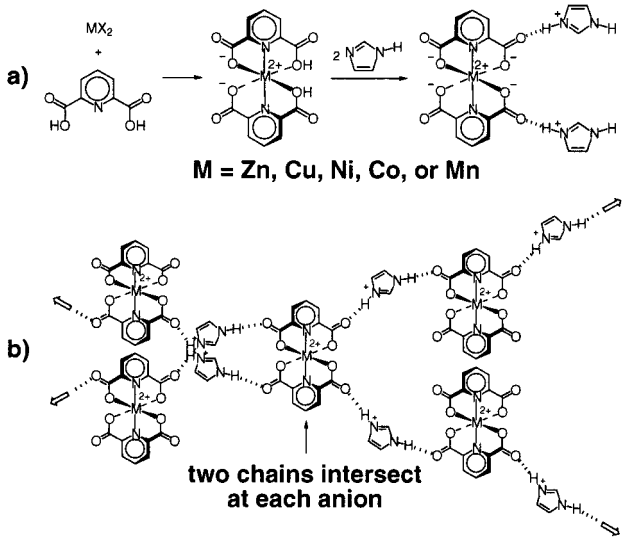

Figure 2. (a) Reaction of MX_2 (M = Mn, Co, Ni, Cu, or Zn; X = Cl or Br) with 2,6-pyridinedicarboxylic acid and imidazole gives the corresponding bis(imidazolium 2,6-pyridinedicarboxylate)metal(II) complexes (**1**−**5** respectively). (b) Two hydrogen-bonded chains of imidazolium cations and carboxylate anions that intersect at the anions.

Despite minor differences in the molecular geometry of the anions, the metal complexes have similar crystal packing. All of the metal complexes crystallize in the same space group (*P*2/*c*) and have unit cells with dimensions and volumes that differ at most by 0.55 Å (6.5%) and 28.5 Å^3 (2.5%), respectively. Packing in these solids is dominated by hydrogen bonding between imidazolium cations and carboxylate anions. Anions of the metal complex are joined to imidazolium cations by ionic $^+$N−H···O$^-$ hydrogen bonds. The four carboxylate groups of the anions are oriented in a flattened tetrahedral arrangement around the metal. Consequently, each anion participates in the formation of two perpendicular chains that intersect at the anions. The resulting network of cross-linked chains forms layers as anticipated. A space-filling model of one layer from the crystal structure of **4** is shown in Figure 4. The hydrogen-bonded layers formed in crystals of **1**−**3** and **5** are nearly identical in structure to those in **4** and are not shown.

The surface of a single hydrogen-bonded layer **4** (and **1**−**3** and **5**) is not flat but corrugated. Each layer forms a grid of cations and anions that contains cavities between the ions; the distance between metal atoms is 13.7 Å by 13.7 Å along the

(51) MacDonald, J. C.; Dorrestein, P. C.; Pilley, M. M. *Cryst. Growth Design* **2000**, *1*, 29−38.
(52) Aakeröy, C. B.; Hitchcock, P. B.; Seddon, K. R. *J. Chem. Soc., Chem. Commun.* **1992**, 553−555.
(53) Aakeröy, C. B.; Hitchcock, P. B. *Acta Crystallogr.* **1994**, *C50*, 759−761.
(54) Aakeröy, C. B.; Nieuwenhuyzen, M. *J. Am. Chem. Soc.* **1994**, *116*, 10983−10991.
(55) MacDonald, J. C.; Dorrestein, P. C. *ACA Trans.* **1998**, *33*, 121−131.

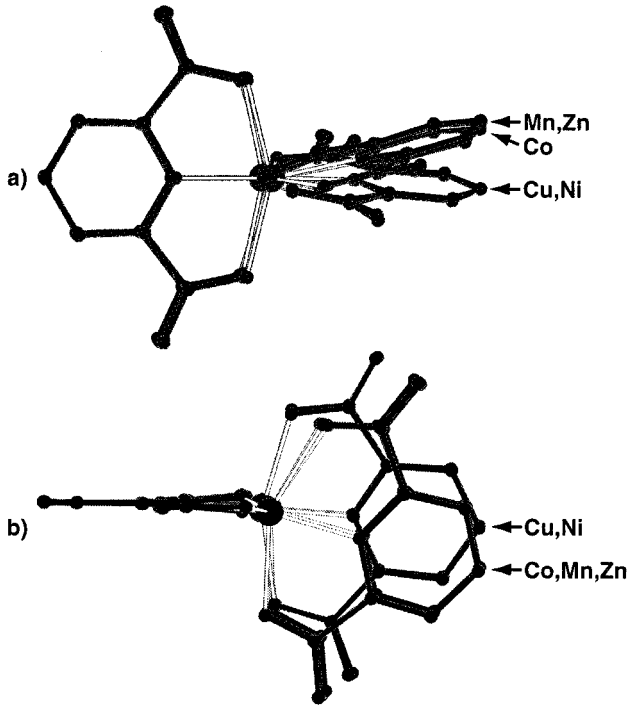

Figure 3. Comparison of the molecular geometries of the anions in **1**−**5**. Differences in structure are illustrated by viewing the pyridyl rings from the side (a) and top (b).

edges of the grid, and 21.5 Å by 16.9 Å along the long and short diagonals of the grid, respectively (Figure 4a). The cavities are not empty in the crystal, but instead are filled by pyridyl rings that protrude from adjacent layers. The fact that the cavities are large enough to accommodate aromatic rings is an attractive feature that we are exploiting in porous materials that selectively trap guest molecules. This packing arrangement places pyridyl rings from neighboring layers on top of one another with a separation of 3.4 Å. Layers stack on top of one another by fitting the bumps of rows on one layer into the hollows between rows on an adjacent layer. A view looking down the *c* axis (001 face) of two layers stacked in this manner is shown in Figure 5d. Views of crystal packing looking down the *a* axis (100 face) and *b* axis (010 face) are shown in Figure 5b,c. These structural features are consistent in all five structures. Given the range of sizes and electronic structures of Mn, Co, Ni, Cu, and Zn, these data suggest that supramolecular layers of this type are likely to form for other transition metals in the 2+ oxidation state as well.

Layers of cations and anions are linked along the direction of stacking (*c* axis) by O−H···O$^-$ hydrogen bonds between molecules of water and carboxylate groups in adjacent layers. Inclusion of water in these structures is not surprising since carboxylate groups are known to form hydrates.[56] The anions in **1**−**5** contain an excess of strong acceptors because each one of the four carboxylate groups can accept at least four hydrogen bonds from donors.[57] Since water has two acidic protons, each molecule can act as a hydrogen-bonding donor twice by bridging between neighboring carboxylate groups. Water also may be included in the lattice simply because there is void space between layers when they stack. Growth of all crystals was achieved by evaporation of solutions of DMSO that were left open to the atmosphere. DMSO is hygroscopic and readily

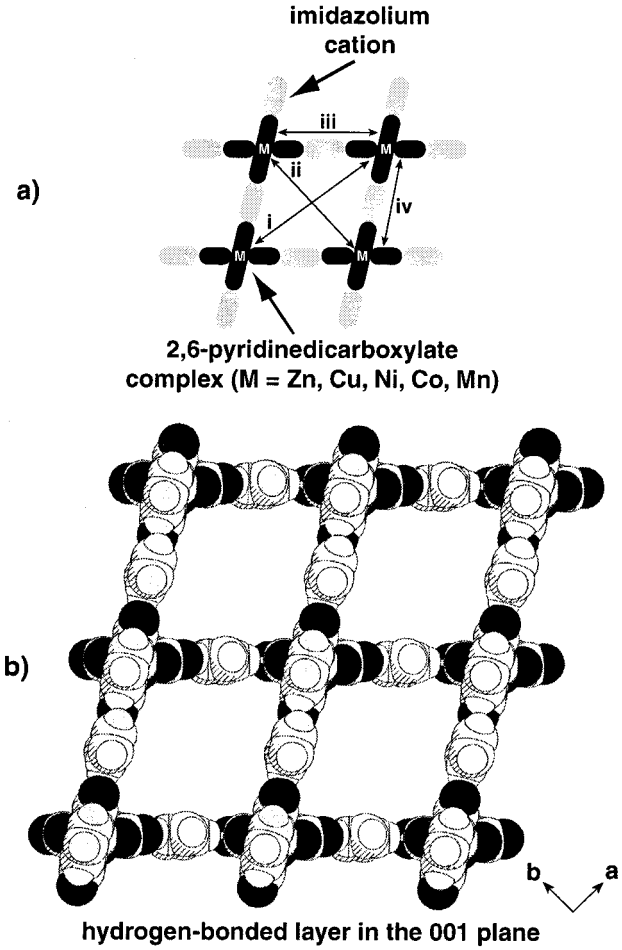

Figure 4. (a) Hydrogen-bonded layer (001 face) of cations and anions formed by the complex with Cu (**4**) shown using a schematic representation. Dimensions of the cavity and spacing of the metal atoms within a layer are indicated by arrows i−iv, which correspond to the following distances: i, 21.5 Å; ii, 16.9 Å; iii , 13.7 Å; iv, 13.7 Å. (b) A space-filling model showing the structure of a single layer of **4**.

absorbs water from the atmosphere. We did not attempt to exclude water by growing crystals under anhydrous conditions. In fact, crystals of **3** and **4** grow with the same crystal structure but different morphology from solutions in 1:1 water/DMSO and also in pure water. Although we did not anticipate that water would be included in the structures of **1**−**5**, the presence of water does not obviate our strategy to design layered structures. Molecules of water are not involved as a structural component within layers; rather, all hydrogen bonds with water occur between adjacent layers.

Mixed Crystals. The similarity between crystal packing in structures containing 2,6-pyridinedicarboxylic acid, imidazole, and 2+ transition metals (Mn^{2+}, Co^{2+}, Ni^{2+}, Cu^{2+}, and Zn^{2+}) suggested that the hydrogen-bonded network of organic ligands would serve as a host lattice in which one metal could be replaced by another metal without disturbing the lattice. This type of material, which we refer to as a mixed crystal, contains a mixture of two or more different types of transition metals within the same crystal. Mixed crystals represent a new class of materials that should exhibit properties that can be altered systematically as a function of the types and relative ratios of transition metals that are present. Manipulation of physical properties in this manner is analogous to the manner in which the conductivity of semiconductors is modulated by doping. Moreover, mixed crystals should have properties such as index

(56) Jeffrey, G. A.; Saenger, W. *Hydrogen Bonding in Biological Structures*; Springer-Verlag: Berlin, Heidelberg, New York, 1991.

(57) Görbitz, C. H.; Etter, M. C. *J. Am. Chem. Soc.* **1992**, *114*, 627−631.

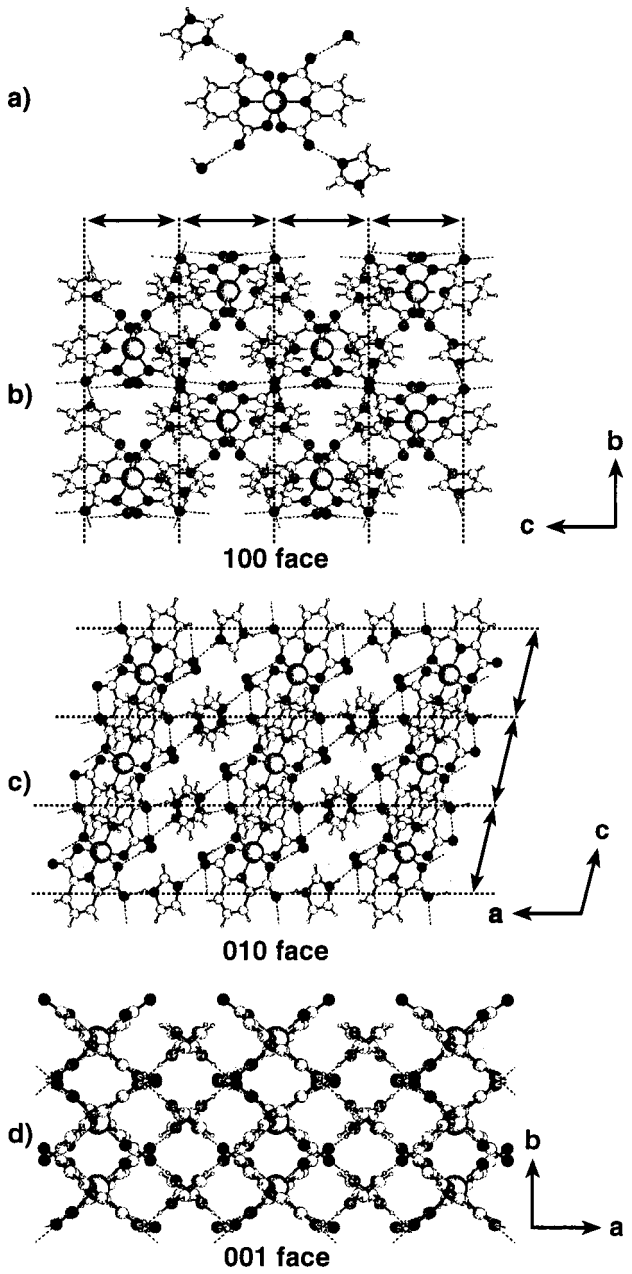

Figure 5. Views of packing in crystals of the complex with Cu (**4**). (a) The molecular structure of **4**. (b) View of the 100 face showing four hydrogen-bonded layers (denoted by double-headed arrows) of cations and anions stacked along the *c* axis. (c) View of the 010 face showing three hydrogen-bonded layers (denoted by double-headed arrows) of cations and anions stacked on top of one another along the *c* axis. (d) View of the 001 face showing two adjacent layers (in the plane of the page) stacked on top of one another.

of refraction and color that can be controlled with a high degree of predictability and precision.

To test the hypothesis that one transition metal can be substituted by another without significantly altering the crystalline lattice, we grew crystals from a series of solutions that contained complexes with two different metals, M_1 and M_2, where M_1 and M_2 were different combinations of Mn^{2+}, Co^{2+}, Ni^{2+}, Cu^{2+}, and Zn^{2+}. The composition of the solutions varied in concentration from 100 mol % of M_1 to 100 mol % of M_2 in 10% molar increments. We anticipated that crystals grown from these solutions would incorporate the two metal complexes in the same relative ratios that were present in solution. In addition, we expected that the color of the crystals would change

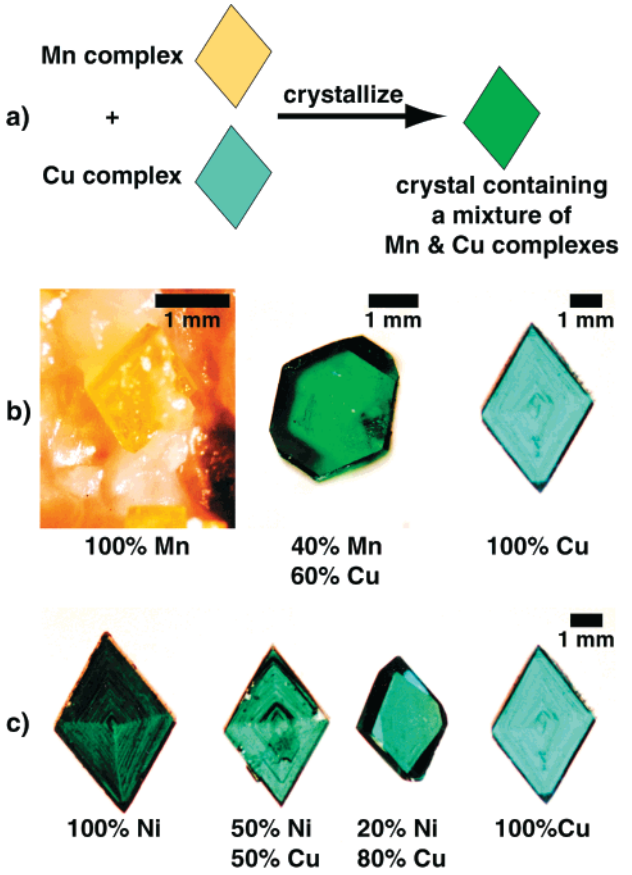

Figure 6. (a) Illustration of a hypothetical mixed crystal (green) grown from a solution that contains complexes of both Mn (yellow) and Cu (blue). (b) Yellow crystals with Mn (left), blue crystals with Cu (right), and green crystals with 40:60 Mn:Cu (center). (c) Green crystals with Ni (left), blue crystals with Cu (right), and blue-green crystals with 50:50 Ni:Cu (left center) and 20:80 Ni:Cu (right center).

incrementally as a function of the concentrations of the metals. Results from using this technique to grow two different mixed crystals are shown in Figure 6. The set of crystals in Figure 6b illustrates how mixing the blue Cu complex (**4**) with the yellow Mn complex (**1**) produced a mixed crystal that is green—a color that reflects the 60:40 ratio of Cu:Mn present in the crystal. Mixed crystals that contain the blue Cu complex (**4**) and the green Ni complex (**3**) in 50:50 and 80:20 ratios, respectively, are shown in Figure 6c. The shift in color from a darker blue-green in the 50:50 crystal to a lighter blue-green in the 80:20 crystal is consistent with the higher relative concentration of Cu. Other examples of mixed crystals are shown in Figure 7. We also have grown one example of a crystal with three components that contained equimolar amounts of the Co, Ni, and Cu complexes (Figure 7d). Analysis by flame atomic absorption spectroscopy or inductively coupled plasmon mass spectrometry of the mixed crystals showed that the relative ratio of the metals in a given crystal was the same as that placed in solution initially. These results suggest that there should be few limitations on the type and number of first-row 2+ transition metals that can be incorporated as mixtures in the host lattice.

To investigate whether the metals are ordered or randomly disordered in the crystal lattice, single crystals composed of mixtures of **3** and **4** were examined using neutron diffraction. Ordering of the metals is possible in the mixed crystals (e.g., segregation of **3** and **4** into alternating layers), but X-ray diffraction cannot readily distinguish between Ni and Cu. Consequently, neutron diffraction on single crystals grown from

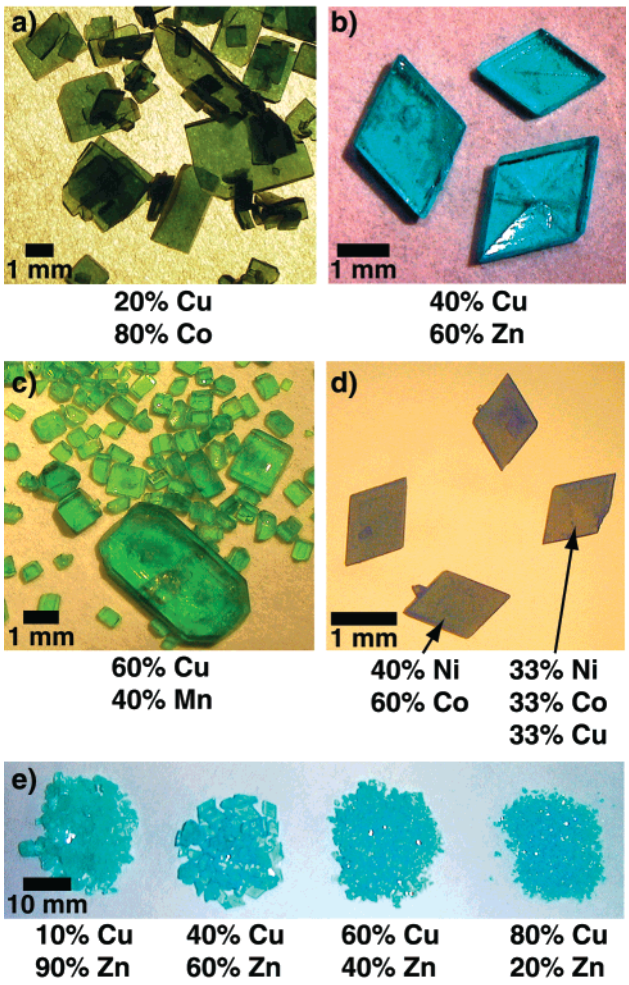

Figure 7. Mixed crystals of (a) 20:80 Cu:Co, (b) 40:60 Cu:Zn, (c) 60:40 Cu:Mn, (d) 40:60 Ni:Co, and 33:33:33 Ni:Co:Cu. The series of mixed crystals in panel e shows a series of crystals with 10:90, 40:60, 60:40, and 80:20 Cu:Zn.

solutions that contained **3** and **4** in 50:50 and 20:80 ratios, respectively, was used to determine the relative ratio of Ni to Cu, and to identify potential ordering of the metal centers. The large difference in neutron scattering lengths between Ni and Cu, 1.03(1) $\times$ 10^{-12} and 0.7718(4) $\times$ 10^{-12} cm, respectively, is more than adequate to distinguish the two metal atoms.[58] Ordering of the metal atoms would have been the most interesting result, but analysis of the neutron diffraction data did not reveal any violations of the space group (*P*2/*c*), or any diffuse reflections indicating the presence of super symmetry. Ni and Cu appear to be mixed, or disordered, on the same site in the lattice, and have a relative ratio corresponding to the solutions from which they were crystallized. Refinement on the occupancy at the metal centers indicated 54:46(4)% and 25:75(3)% of Ni and Cu, respectively. While there is no evidence that ordering of **3** and **4** has occurred, these results cannot confirm that ordering has not occurred. For example, it is possible that **3** and **4** segregate into homogeneous layers that stack in a random order during crystallization.

The bond distances between transition metals and nitrogen and oxygen atoms on the 2,6-pyridinedicarboxylate ligands are given in Table 1 and plotted in Figure 8 for **1**−**5**, respectively. The decrease in the average distances for Mn, Co, and Ni, followed by an increase in the average distances for Cu and Zn, is consistent with trends observed for hexaaqua dipositive

(58) Sears, V. F. *Neutron News* **1992**, *3*, 26.

Table 1. Comparison of Bond Distances between the Metal (M) and Nitrogen and Oxygen Atoms on the 2,6-Pyridinedicarboxylate Ligand[a]

	M−N1	M−O1	M−O3
Mn (**1**)	2.157(3)	2.223(3)	2.219(3)
Co (**2**)	2.021(1)	2.165(1)	2.152(1)
Ni (**3**)	1.966(1)	2.136(1)	2.121(1)
50:50 Ni:Cu	1.9514(3)	2.1434(4)	2.1728(3)
20:80 Ni:Cu	1.942(1)	2.159(3)	2.186(3)
Cu (**4**)	1.940(1)	2.173(1)	2.208(1)
Zn (**5**)	2.026(2)	2.196(1)	2.166(1)

[a] X-ray diffraction data for crystals of pure **1**−**5** were collected at room temperature, while neutron diffraction data for the mixed crystals of **3** and **4** were collected at 20 K.

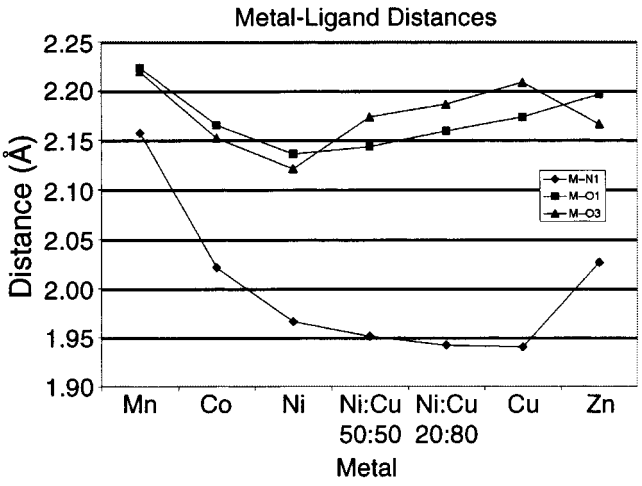

Figure 8. Comparison of the distances between metal atoms (M) and nitrogen (N1) or oxygen atoms (O1 or O3) on 2,6-pyridinedicarboxylate ligands in **1**−**5**.

ions of the first row transition metals.[59] Furthermore, it is clear that a Jahn−Teller distortion is exhibited for Cu^{2+}, which is also consistent with trends observed for first row transition metals.[59] The Jahn−Teller distortion appears to be expressed as an elongation of the M−O3 distance, although static or dynamic (at room temperature) disorder due to elongation of M−O1 or M−O3 at different sites is feasible as well. Superimposed on the possible Jahn−Teller disorder is the disorder of the coordination by Ni and Cu in the mixed crystals. It is interesting to note that the magnitudes of the difference between the M−O1 and M−O3 distances in the crystals that contain Cu are fairly independent of the content of Cu and temperature; the structures with mixtures of Ni and Cu were obtained at 20 K and the structure with pure Cu was obtained at room temperature.

The thermal ellipsoids from the neutron structures were analyzed in more detail for evidence of disorder by evaluating the difference in mean-square displacement amplitudes (ΔMSDA) between pairs of atoms along their interatomic vectors.[60,61] For rigid bonds, the MSDA values along the interatomic vectors should be equal, such that the difference should be close to zero. In the case of disorder, the ΔMSDA value can be large due to the distribution of the atoms on the ligands over two disordered sites. In the neutron structures of the mixed crystals with 50:50 Ni:Cu and 20:80 Ni:Cu, the ΔMSDA values for the two metal−

(59) Cotton, F. A.; Daniels, L. M.; Murillo, C. A.; Quesada, J. F. *Inorg. Chem.* **1993**, *32*, 4861−4867.

(60) Dunitz, J. D.; White, D. N. J. *Acta Crystallogr. A* **1973**, *29*, 93−94.

(61) Schomaker, V.; Trueblood, K. N. *Acta Crystallogr. B* **1968**, *24*, 63−76.

oxygen bonds (M−O1 and M−O3) around the metal atoms are significantly larger than the ΔMSDA values for M−N1. The values for 50:50 Ni:Cu and 20:80 Ni:Cu (in parentheses) are M−N1 = 3(−8) × 10^4 Å^2, M−O1 = 12(24) × 10^4 Å^2, and M−O3 = 32(30) × 10^4 Å^2. This result could arise from the difference in bond distances with Ni versus Cu, or from disorder in the direction of the Jahn−Teller distortion. The ΔMSDA values between metal and nitrogen atoms are small and are reflected in the small change in bond distance as the content of metal changes from Ni to Cu. These data suggest that disorder does not affect the nitrogen donor atom. The metal−nitrogen bond is not affected by the Jahn−Teller distortion in the crystals that contain Cu. Output from this analysis is provided in the Supporting Information.

It should be noted that mixed crystals were formed using two different procedures (A and B) that had the potential to yield different crystalline products. As described in the Experimental Section, synthesis and crystallization of pure **1**−**5** using procedure A was carried out in one pot by mixing 2,6-pyridinedicarboxylic acid, imidazole, and a metal halide salt in DMSO in a 4:4:1 relative molar ratio, respectively, followed by crystallization of these complexes by slow evaporation from the same solution. The resulting metal complexes contained 2,6-pyridinedicarboxylic acid, imidazole, and a metal salt in DMSO in a 2:2:1 relative molar ratio, respectively (Figure 2). Mixed crystals were grown using this same technique (procedure A) by dissolving a mixture of two different metal halide salts instead of a single metal halide salt. Since the rate at which the metal complexes form varies for different metals, it is possible that the ratio of different metal complexes incorporated into a given mixed crystal may vary depending on the rate at which crystals nucleate and grow. For example, consider the case in which a complex with one metal, M_1, forms at a faster rate than a complex with a second metal, M_2. If crystals of M_1 begin to nucleate and grow at a rate that is fast relative to the formation of M_2 in solution, the crystal should incorporate a higher percentage of M_1 relative to M_2.[62] If crystals of M_1 nucleate and grow at a rate that is comparable to or slower than the formation of M_2 in solution, the crystals should incorporate M_1 and M_2 statistically as a function of the relative molar ratio of M_1 and M_2 introduced into the solution. All of the mixed crystals grown using procedure A that we analyzed contained the two metal complexes in the same relative molar ratios placed in solution. This result suggests that the metal complexes form in solution at a rate that is fast relative to the nucleation and growth of single crystals, which is not surprising considering that single crystals visible to the naked eye generally did not appear in solution until at least 24 h after mixing the components in solution.

Mixed crystals also were grown by dissolving mixtures of two different metal complexes in solution (procedure B) using pure metal complexes formed prior to dissolution. Since this method did not involve synthesis of the metal complexes in the same solution from which the crystals were grown, the kinetics for the formation of the different complexes was not a factor. Previous research has shown that the morphology of organic crystals often changes when crystals are grown in the presence of even small amounts of impurities or additives.[63] It is interesting to note that the morphology of mixed crystals grown using procedure B was the same as that of mixed crystals grown using procedure A when the same solvent (i.e., DMSO) was used. The fact that the morphology did not change is surprising considering that 2,6-pyridinedicarboxylic acid and imidazole were present in 2-fold excess when procedure A was used, but were not present in excess when procedure B was used.

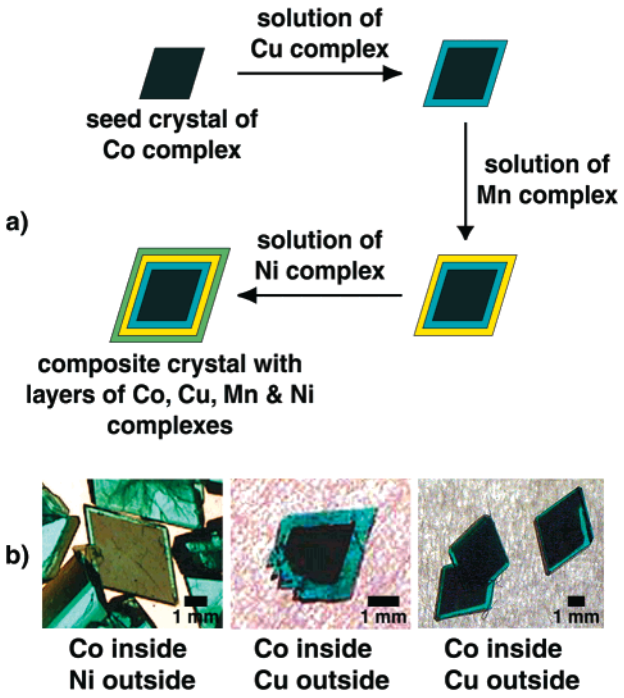

Figure 9. (a) Illustration of a hypothetical composite crystal in which successive layers of different metal complexes are added sequentially to the surface of a seed crystal. (b) Actual crystals composed of an inner region of **2** and outer regions of **3** (left) or **4** (center and right).

Composite Crystals. Growth of thin films of materials is one of the more important and fast growing areas of research in the development of a wide range of materials (e.g., liquid crystals, polymers, coatings, optical waveguides, and magnetic media). We are working to develop a technique to make single-crystal films based on our layered metal complexes. Our approach takes advantage of the close structural match between the lattices in the crystals of **1**−**5**. A crystal of one metal complex as a substrate, or seed, was used to nucleate and grow a layer of a different metal complex epitaxially on the surface. This concept is illustrated in Figure 9a. Two examples of composite crystals composed of two different metal complexes are shown in Figure 9b. These crystals formed when seed crystals of the cobalt complex (**2**) were placed into a solution in DMSO that contained either the Ni complex (**3**) or the Cu complex (**4**). Epitaxial growth of a new layer on the seed crystal of **2** produced composite crystals with fast, uniform growth of an outer layer of **3** or **4** along the directions of hydrogen bonding in the seed crystal of **2**, which run parallel to the large diamond-shaped 001 face (in the plane of the page) in Figure 9. Epitaxial growth occurs more slowly on the 001 face, which corresponds to the surface on which layers stack during the growth of crystals. The morphology and aspect ratio of the crystalline material that forms the epitaxial regions of the composite crystal are commensurate with those of the underlying seed crystals. Although we have demonstrated epitaxial deposition of just one new layer of a different complex, we are working to develop a technique to grow many successive crystalline layers that contain different metals.

(62) Palmore, G. T. R.; Luo, T.-J. M.; Martin, T. L.; McBride-Wieser, M. T.; Voong, N. T.; Land, T. A.; DeYoreo, J. J. *ACA Trans.* **1998**, *33*, 45−57.

(63) Addadi, L.; Berkovitch-Yellin, Z.; Weissbuch, I.; Mil, J. V.; Shimon, L. J. W.; Lahav, M.; Leiserowitz, L. *Angew. Chem., Int. Ed. Engl.* **1985**, *24*, 466−485.

Table 2. Collection of X-ray Data and Refinement of Crystal Structures for **1**−**5**

compd	**1**	**2**	**3**	**4**	**5**
formula	$C_{20}H_{20}N_6O_{10}Mn$	$C_{20}H_{20}N_6O_{10}Co$	$C_{20}H_{20}N_6O_{10}Ni$	$C_{20}H_{20}N_6O_{10}Cu$	$C_{20}H_{20}N_6O_{10}Zn$
molecular weight	559.38	563.37	563.13	567.96	569.83
crystal system	monoclinic	monoclinic	monoclinic	monoclinic	monoclinic
space group	*P*2/*c*	*P*2/*c*	*P*2/*c*	*P*2/*c*	*P*2/*c*
crystal	yellow blocks	red-brown prisms	green prisms	blue prisms	colorless prisms
a (Å)	8.931(2)	8.996(2)	10.596(1)	10.753(1)	8.8461(1)
b (Å)	10.340(2)	10.302(2)	8.588(1)	8.449(1)	10.419(1)
c (Å)	12.580(3)	12.385(3)	12.803(1)	12.840(1)	12.315(1)
α (deg)	90	90	90	90	90
β (deg)	93.00(3)	93.31(3)	103.764(1)	103.628(1)	92.244(7)
γ (deg)	90	90	90	90	90
V (Å^3)	1160.1(4)	1145.9(4)	1131.7(1)	1133.6(1)	1134.2(2)
Z	2	2	2	2	2
D_{calc} (g/cm^3)	1.601	1.633	1.653	1.664	1.668
F(000)	574	578	580	582	584
μ(Mo Kα) (mm^{-1})	0.639	0.819	0.929	1.035	1.154
temp (K)	293(2)	293(2)	293(2)	293(2)	293(2)
θ−2*θ* scans; *θ* range (deg)	1.97−22.50	1.98−31.53	1.98−27.88	1.95−27.93	2.30−25.00
no. of reflcns collected	5421	6524	6464	6888	2267
no. of unique reflcns	1520	3144	2647	2665	2001
no. of obsd reflcns ($I > 2\sigma(I)$)	978	2721	2381	2415	1873
no. of parameters	184	184	176	176	184
data/parameters (obsd reflcns)	5.32	13.53	13.53	13.72	10.18
R/wR^2 (obs data)[a]	0.042/0.073	0.033/0.091	0.027/0.070	0.028/0.073	0.025/0.066
R/wR^2 (all data)[a]	0.084/0.086	0.039/0.094	0.031/0.073	0.031/0.074	0.027/0.068
$\Delta\rho_{max/min}$ (e/Å^{-3})	0.29/−0.29	0.51/−0.32	0.29/−0.50	0.33/−0.58	0.34/−0.23
S	0.943	1.074	1.045	1.058	1.096

[a] $R = \sum(||F_o| - |F_c||)/\sum|F_o|$; $wR^2 = [\sum w(|F_o| - |F_c|)^2/\sum w(F_o)^2]^{1/2}$.

Optical polarizing microscopy showed that the inner and outer regions of these composite crystals extinguish light uniformly under crossed polarizing lenses. This behavior indicates that composite crystals behave as single crystals rather than as a mosaic of two different, or twinned, crystals that have different orientations. X-ray powder diffraction (XPD) traces of crystalline samples cut from the outer epitaxial region of a composite crystal grown on a seed crystal of **2** from a solution of **4** were identical to XPD traces obtained from crystals of pure **4**. These results confirm that the epitaxial layer of **4** crystallizes in the same crystalline phase present in pure crystals of **4**. Moreover, these results demonstrate that small differences in the lattice energies of **2** and **4** caused by slight mismatches in the dimensions of the lattices (Table 2) or by small differences in molecular geometry (Figure 3) do not create enough stress at the interface between **2** and **4** to prohibit epitaxial growth, or to promote nucleation of a new polymorph. Consequently, composite crystals behave as a uniform, continuous crystalline phase. To our knowledge, these crystals represent the first examples of composite crystalline materials composed of organic molecules and transition metals. We currently are studying the process of crystallization of these materials to understand how to control growth of composite crystals precisely. Ultimately, we want to develop a methodology that will enable us to generate composite materials composed of many different epitaxial layers and to control the thickness of individual layers.

How Similar Are the Crystal Structures of 1−5? One of our goals was to address the question of how similar the crystal structures of different compounds must be to be considered as having identical or nearly identical structures? This question is important in the context of crystal engineering with regard to the design of materials such as mixed and composite crystals that require a close match between the molecular packing and lattice energies of the individual components. As shown in Table 2, the dimensions of the unit cells of **1**−**5** are similar, yet there is some disparity between the structures. For example, the dimensions of the *a* and *b* axes switch on going from the structures of **1**, **2**, and **5** to those of **3** and **4.** In addition, the angle *β* in **3** and **4** (103.6−103.8°) widens by 10° relative to that in **1**, **2**, and **5** (92.2−93.3°). This increase in *β* correlates with more nearly linear N−M−N (M = Mn^{2+}, Co^{2+}, Ni^{2+}, Cu^{2+}, or Zn^{2+}) angles in the anions in **3** and **4**, as shown in Figure 3. The increase in *β* and change in molecular geometry in **3** and **4** has almost no effect on the structure and spacing within individual hydrogen-bonded layers; rather, widening of the angle is manifested by small changes in the distances that metal centers are offset as adjacent layers stack on top of one another. From the viewpoint of crystal engineering, the supramolecular structure of the layers in **1**−**5** is relatively constant, while changes in crystalline structure that arise from packing of the layers are minor and insignificant. Evidence that differences in packing are inconsequential is 2-fold. First, if the molecular packing or lattice energies in **3** and **4** were significantly different than those in **1**, **2**, and **5**, it is likely that mixed crystals that contain combinations of these complexes would not form at all, or that there would be ordering or segregation of the metal complexes. Second, it is likely that composite crystals that contain combinations of **3** or **4** and **1**, **2**, or **5** would not form. The greatest chance of a mismatch in molecular packing or lattice energies should occur when an attempt is made to grow an epitaxial layer of **3** or **4** on a seed crystal of the other metal complexes. The composite crystals shown in Figure 9 feature epitaxial layers of **3** or **4** grown on the surface of seed crystals of **2**. Optical microscopy indicates that there is no macroscopic mismatch, and that the composite crystals appear to behave optically as single crystals at the interface between the two metal complexes. Consequently, the data suggest that supramolecular structure of the layer motif formed in **1**−**5** is robust and flexible enough to accommodate perturbations in molecular structure and in the packing of layers without significantly altering bulk crystalline structure.

Magnetic Properties of Crystals of 3, 4, and 50:50 3:4. The dc magnetization of crystals of the Ni complex (**3**), the Cu complex (**4**), and a mixed crystal containing **3** and **4** in a 50:50

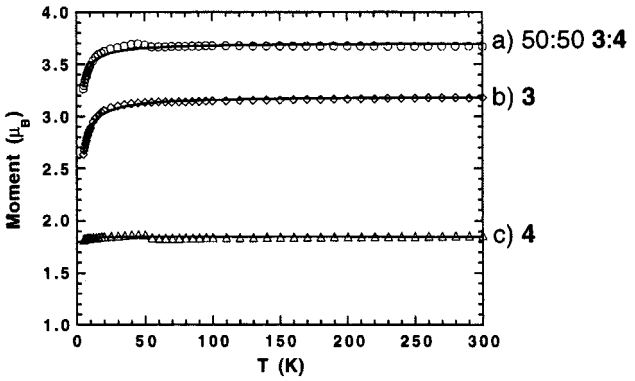

Figure 10. Temperature-dependence of the effective magnetic moment for (a) 50:50 **3**:**4**, (b) **3**, and (c) **4**.

ratio (50:50 **3**:**4**) was measured between 5 and 300 K and the results are shown collectively in the form of $\mu_{eff}(T)$ in Figure 10. Fitting of the data to a Curie−Weiss expression yielded Lande *g*-values of 2.17(1), 2.25(1), and 2.14(1) and small Weiss constants, θ, of −1.63(2), −2.20(9), and −0.17(1) K for 50:50 **3**:**4**, **3**, and **4**, respectively. The effective moments are 3.18 and 1.86 μ_B at 300 K for **3** and **4**, respectively, while that of 50:50 **3**:**4** is 3.67 μ_B. In all cases, the moments at room temperature exceed the spin-only values of 1.78, 2.83, and 3.35 μ_B for $S = {}^1/_2$, 1, and ${}^3/_2$ ($S_{total} = 1 + {}^1/_2$ for 50:50 **3**:**4**), respectively, due to the anisotropy of the *g*-values of these ions. The magnetic moments remain constant upon cooling to ∼50 K. Further cooling to 5 K yields a gradual decrease of $\mu_{eff}(T)$, which is attributed to the zero-field splitting of the Ni(II) $^3A_{2g}$ ground state[64] and very weak antiferromagnetic interactions between adjacent metal sites in 50:50 **3**:**4** and **3**. This contrasts with the magnetic behavior of **4**, which shows a temperature-independent magnetic moment over the measured temperature range. Using a mean-field theory,[64] eq 1 , exchange coupling constants, J/k_B,

$$\left|\frac{J}{k_B}\right| = \frac{3\theta}{2zS(S+1)} \qquad (1)$$

of −0.11 (50:50 **3**:**4**), −0.28 (**3**), and −0.06 K (**4**) were obtained assuming the number of magnetic nearest-neighbors (*z*) is 6. As the low-temperature data likely consist of two parameters, a true θ and *D*, the θ-value obtained from the Curie−Weiss fit must be viewed with caution; thus the seemingly larger *J*-value found for both 50:50 **3**:**4** and **3** may be overestimated. These results demonstrate that crystals of **1**−**5** show no long-range magnetic ordering, which is not surprising considering the large separations, and, consequently, weak exchange interactions between the metal atoms in these materials. Although we did not expect these crystals to show magnetic behavior, these data will serve as a baseline to compare with the magnetic behavior of new types of related crystalline materials that we are investigating presently.

Conclusions

We have shown that bis(imidazolium 2,6-pyridinedicarboxylate)M(II) complexes **1**−**5** serve as supramolecular building blocks that form extended layers that have a single, well-defined, predictable structure in the solid state. These layers pack in a predictable arrangement to form a robust host lattice that accommodates at least five different transition metals without significantly altering molecular packing. Consequently, this layer motif serves as a platform with which to control molecular packing by design for engineering the structures, and, ultimately, the properties of crystals. The crystalline solids of **1**−**5** represent a new class of modular materials in which the organic ligands serve as a structural component that defines a single packing arrangement that persists over a range of structures, and in which the metal serves as an interchangeable component. This type of supramolecular modularity is a crucial element for engineering useful materials because it provides a handle with which to alter the physical properties of a material without changing the structure of the material. This concept is analogous to the way in which the properties of copolymers are modified at the molecular level by altering the molecular structure of just one of a pair of monomeric starting materials. We have demonstrated the utility of this modular approach at the supramolecular level through the design of mixed and composite crystals, which to our knowledge represent the first examples of such unique materials.

We are expanding our research presently to investigate new types of crystalline materials constructed with ligands that contain two 2,6-pyridinedicarboxylic acid groups rather than a single 2,6-pyridinedicarboxylic acid group. Use of these tetracarboxybispyridyl ligands will provide the means to link metal centers in adjacent layers covalently, and thus to control the alignment and spacing between layers. We expect that this strategy will allow for complete control over molecular packing in three dimensions, and should provide a new avenue for the deliberate design of novel porous and optical materials.

Experimental Section

General Techniques. Manganese(II) chloride tetrahydrate, cobalt(II) bromide, nickel(II) bromide, copper(II) bromide, zinc(II) bromide, 2,6-pyridinedicarboxylic acid, and imidazole were purchased from Aldrich or Acros. All chemicals were used as received without further purification. IR samples were prepared as mulls in Nujol. IR spectra were obtained on a Nicolet Avatar 360 FT-IR instrument. Melting point data were collected with a Meltemp instrument and are uncorrected. Differential scanning calorimetry data were collected using a Mettler FP 85 TA cell and FP 90 central processor and heating at 10 °C/min. XPS data were collected using a Kevex Sigma II instrument. The relative molar ratios of different transition metals in mixed crystals were determined using a Perkin-Elmer 56 flame atomic absorption spectrometer or a Sciex ELAN inductively coupled plasmon mass spectrometer. X-ray powder diffraction data were collected on a Siemens/Bruker D-500 powder X-ray diffractometer.

General Method to Synthesize and Crystallize Bis(imidazolium 2,6-pyridinedicarboxylate)metal(II) Complexes (1−5). The following general procedure was used to synthesize and grow crystals of bis(imidazolium 2,6-pyridinedicarboxylate)metal(II) complexes with Mn^{2+}, Co^{2+}, Ni^{2+}, Cu^{2+}, or Zn^{2+}. 2,6-Pyridinedicarboxylic acid (e.g., 4.500 g, 26.93 mmol) and imidazole (e.g., 1.833 g, 26.93 mmol) were dissolved in 400 mL of DMSO with stirring at approximately 40 °C for 30 min. The appropriate metal chloride or bromide salt (e.g., 1.504 g, 6.733 mmol) was then added and the solution warmed and stirred until all solids disappeared and the solution turned clear. The solution was cooled to room temperature and left uncovered. Single crystals of bis(imidazolium 2,6-pyridinedicarboxylate)metal(II) dihydrate formed as clear, colored prisms in solution after several days. Single crystals were removed from solution and dried on filter paper.

It should be noted that formation of metal complexes and subsequent growth of single crystals was achieved by mixing 2,6-pyridinedicarboxylic acid, imidazole, and metal in DMSO in a 4:4:1 relative molar ratio, respectively, while crystals of metal complexes grown from these solutions contained the three components in a 2:2:1 relative molar ratio, respectively. Addition of an excess of 2,6-pyridinedicarboxylic acid and imidazole relative to the metal was determined experimentally as the optimal ratio of the components to grow large, well-developed single crystals. This protocol was established on the basis of a series of experiments involving synthesis and crystallization of the complexes

(64) Carlin, R. L. *Magnetochemistry*; Springer-Verlag: New York, 1986.

by slow evaporation from solutions of DMSO in which the relative concentrations of the three components were varied systematically. Starting from a 1:1:1 relative ratio of 2,6-pyridinedicarboxylic acid, imidazole, and metal, the concentration of the individual components was increased incrementally up to a 20-fold excess relative to the other two components. The concentration of pairs of components was also increased incrementally keeping the relative concentration of the pairs equal. Large, single crystals of the metal complexes formed when the ratio of 2,6-pyridinedicarboxylic acid to imidazole was equal, and when the relative ratio of 2,6-pyridinedicarboxylic acid, imidazole, and the metal varied between 2.4:2.4:1 and 5.1:5.1:1, respectively. The optimal relative ratio of 2,6-pyridinedicarboxylic acid, imidazole, and metal was determined empirically to be 4:4:1, respectively. Microcrystalline powders formed in solution when the relative ratio of 2,6-pyridinedicarboxylic acid and imidazole fell outside of this range. We have not yet determined why large, well-developed, single crystals form when an excess of 2,6-pyridinedicarboxylic acid and imidazole is present in solution.

Growth of Mixed Crystals. The following two general procedures were used to synthesize and grow mixed crystals that contained complexes between 2,6-pyridinedicarboxylic acid, imidazole, and mixtures of two different transition metals. Typical experiments were set up as follows. **Procedure A:** 2,6-Pyridinedicarboxylic acid (e.g., 4.500 g, 26.93 mmol) and imidazole (e.g., 1.833 g, 26.93 mmol) were dissolved in 400 mL of DMSO with stirring at approximately 40 °C for 30 min. A pair of metal(II) salts was added such that the total combined concentration of both metals was one-fourth that of 2,6-pyridinedicarboxlic acid and imidazole (e.g., 1.504 g, 6.733 mmol). The solution was then warmed and stirred until all solids disappeared and the solution turned clear. The solution was cooled to room temperature and left uncovered. **Procedure B:** Equimolar amounts of two different metal complexes prepared previously (using the general method to synthesize and crystallize pure bis(imidazolium 2,6-pyridinedicarboxylate)metal(II) complexes described above) were placed in a beaker and DMSO was added with stirring at room temperature until all solids dissolved. The solution was left uncovered. Single mixed crystals of the complexes formed as clear colored prisms in solution after several days using either procedure, although procedure B generally gave smaller single crystals of poorer quality. Single mixed crystals were removed from solution and dried on filter paper. It should be noted that 2,6-pyridinedicarboxylic acid, imidazole, and the metal are present in solution in a 4:4:1 ratio when procedure A was used, and in a 2:2:1 ratio when procedure B was used. Series of mixed crystals that contained pairs of metals, M_1 and M_2, were grown from solution using procedure A or B with different combinations of Mn^{2+}, Co^{2+}, Ni^{2+}, Cu^{2+}, and Zn^{2+}. The composition of the solutions varied in concentration from 100 mol % of M_1 to 100 mol % of M_2 in 10% molar increments. Incorporation of complexes that contained both metals was evident in each case by the color of the mixed crystals. For example, the crystals that contained the yellow manganese complex (**1**) and the blue Cu complex (**4**) were green in color. Analysis of the content of metal was carried out using either flame atomic absorption spectroscopy or inductively coupled plasmon mass spectroscopy.

Growth of Composite Crystals. Composite crystals that contained **2** and either **3** or **4** were grown using the same procedure used to form crystals of pure **1**−**5** described previously. The following procedure describes how composite crystals composed of **2** and **3** were grown. The same procedure was also used to grow composite crystals composed of **2** and **4**. A solution was set up to grow pure crystals of **2**. A separate solution was set up to grow crystals of **3**. A seed crystal of **2** was removed from solution carefully with a spatula and placed immediately into the solution in which crystals of **3** were already starting to form. Uninterrupted epitaxial growth of **3** on the surface of the seed crystal of **2** occurred using this method. When seed crystals of **2** were placed into a solution of **3** in which crystals of **3** had not yet begun to grow, the seed crystal of **2** either dissolved completely or dissolved partially followed by epitaxial growth of **3**, depending on how close the solution of **3** was to saturation.

Determination of X-ray Crystal Structures. Single-crystal X-ray diffraction data were collected on a Siemens SMART/CCD diffractometer with graphite monochromated Mo Kα radiation and equipped with an LT-II low-temperature device. Diffracted data were corrected for absorption using the SADABS program. SHELXS-86 and SHELXL-93 software were used to solve and refine structures on an SGI O2 UNIX platform. Refinement was based on F^2. All non-hydrogen atoms were refined anisotropically. Hydrogen atoms on heteroatoms were located and refined with isotropic thermal parameters. The remaining hydrogen atoms were fixed in calculated positions and refined isotropically with thermal parameters based upon the corresponding attached carbon atoms [$U(H) = 1.2U_{eq}(C)$]. Selected crystallographic data are available as Supporting Information (supplementary Tables 1−25).

Determination of Neutron Crystal Structures. The samples were wrapped in aluminum foil, glued to an aluminum pin, and mounted on the Single-Crystal Diffractometer (SCD) at the Intense Pulsed Neutron Source (IPNS) at Argonne National Laboratory. The crystals were cooled to 20 K with a Displex closed-cycle helium refrigerator. Thirty-five individual histograms were collected for the crystal of 50:50 **3**:**4**. Twenty-six individual histograms were collected for the crystal of 20:80 **3**:**4**. Approximately two octants of data (h, k, $\pm l$) were collected for each crystal. Bragg reflections in each histogram were integrated and corrected for the Lorentz factor and the incident spectrum.[65,66] A wavelength-dependent spherical absorption correction was applied, but reflections related by symmetry could not be averaged because of the dependence of extinction on wavelength.[67] The positions of atoms from the X-ray structure of the pure **4** were used as a starting point in the refinement. The atoms of Cu and Ni were refined on the same position with their total occupancies constrained to be fully occupied. The positions of atoms and anisotropic thermal parameters of the other atoms were allowed to refine as usual. The refinements were performed with the GSAS program.[68] Collection of data and refinement parameters are summarized in the Supporting Information in Table 26. The positions of atoms, anisotropic thermal parameters, pertinent distances and angles of covalent bonds, and distances and angles of hydrogen bonds are given in the Supporting Information in Tables 27−31, respectively.

Magnetic Measurements. DC magnetization measurements were carried out between 2 and 300 K utilizing a Quantum Design MPMS-2 7 T SQUID magnetometer. Powdered samples of **3**, **4**, or 50:50 **3**:**4** weighing ∼100 mg were loaded into gel caps, mounted in a clear plastic straw, and attached to the end of the sample rod. Samples were inserted into the instrument at 100 K and cooled in zero-field to 5 K where the dc field was then charged to 0.1 T and data collected on warming. Each recorded data point was the average of four individual measurements obtained using a 4 cm scan length. All magnetic data were corrected for core diamagnetism as calculated from Pascal's constants.

Thermal Behavior of 1−5. Upon heating in a Meltemp melting point instrument, crystals of **1**−**5** all fractured and turned opaque between 80 and 100 °C, followed by decomposition between 250 and 280 °C. Differential scanning calorimetry showed either two or three endothermic peaks for **1**−**5**. The last of these peaks corresponds to the decomposition of crystals observed above. The first peak or two peaks most likely correspond to loss of water from the lattice.

Bis(imidazolium 2,6-pyridinedicarboxylate)manganese(II) Dihydrate (1). Crystals: clear yellow blocks. IR (cm^{-1}): 3485, 3388, 3275, 3132, 3108, 3067, 2728, 2643, 2573, 1900, 1617, 1568, 1427, 1281; DSC (10 °C/min, T-onset, °C): 138.8, 156.9, 266.8.

Bis(imidazolium 2,6-pyridinedicarboxylate)cobalt(II) Dihydrate (2). Crystals: clear dark reddish brown prisms. IR (cm^{-1}): 3482, 3374, 3284, 3139, 3109, 2776, 2649, 2649, 2583, 2162, 1896, 1618, 1572, 1425, 1395, 1285; DSC (10 °C/min, T-onset, °C): 154.3, 165.3, 259.8.

Bis(imidazolium 2,6-pyridinedicarboxylate)nickel(II) Dihydrate (3). Crystals: clear green prisms or blocks. IR (cm^{-1}): 3487, 3409, 3076, 2718, 2651, 1616, 1572, 1420, 1280; DSC (10 °C/min, T-onset, °C) 188.9, 280.3.

(65) Schultz, A. J.; Srinivasan, K.; Teller, R. G.; Williams, J. M.; Lukehart, C. M. *J. Am. Chem. Soc.* **1984**, *106*, 999.
(66) Schultz, A. J. *Trans. Am. Crystallogr. Assoc.* **1987**, *23*, 61.
(67) Howard, J. A. K.; Johnson, O.; Schultz, A. J.; Stringer, A. M. *J. Appl. Crystallogr.* **1987**, *20*, 120.
(68) Larson, A. C.; Dreele, R. B. V. Los Alamos National Laboratory, Los Alamos, 1994.

Bis(imidazolium 2,6-pyridinedicarboxylate)copper(II) Dihydrate (4). Crystals: clear blue prisms. IR (cm^{-1}): 3494, 3417.61, 3250, 3129, 3110, 2653, 1620, 1420, 1279; DSC (rate 10 °C/min, T-onset, °C): 188.7, 253.3.

Bis(imidazolium 2,6-pyridinedicarboxylate)zinc(II) Dihydrate (5). Crystals: colorless prisms or blocks. IR (cm^{-1}): 3485, 3377, 3140, 3108, 3076, 2647, 1896, 1622, 1584, 1572, 1428, 1395.

Acknowledgment. The author thank the donors of the Petroleum Research Fund, administered by the American Chemical Society, for support of this research at Northern Arizona University (No. 34605-B3). The work at Argonne National Laboratory was supported by the U.S. Department of Energy, Basic Energy Sciences-Material Sciences under Contract No. W-31-109-ENG-38. J.C.M. gives special thanks to Mike Zaworotko, Kumar Biradha, and Christer Aakeröy for collecting X-ray data on crystals of **1**−**5**.

Supporting Information Available: X-ray crystallographic data are given in Tables S1−S25 (PDF) and in CIF files for **1**−**5**. Neutron crystallographic data are given in Tables 26−33 for crystals of 20:80 **3**:**4** and 50:50 **3**:**4** (PDF). This material is available free of charge via the Internet at http://pubs.acs.org.

JA002102V